

BeppoSAX observations of three distant, highly luminous clusters of galaxies: RXJ1347-1145, Z3146 and A2390

S. Ettori, S.W. Allen and A.C. Fabian

Institute of Astronomy, Madingley Road, Cambridge CB3 0HA

27 October 2018

ABSTRACT

We present an analysis of *BeppoSAX* observations of three clusters of galaxies which are amongst the most luminous in the Universe: RXJ1347-1145, Zwicky 3146 and Abell 2390. Using data from both the Low Energy (LECS) and Medium Energy (MECS) Concentrator Spectrometers, and a joint analysis with the Phoswich Detection System (PDS) data above 10 keV, we constrain, with a relative uncertainty of between 7 and 42 per cent (90 per cent confidence level), the mean gas temperature in the three clusters. These measurements are checked against any possible non-thermal contribution to the plasma emission and are shown to be robust.

We confirm that RXJ1347-1145 has a gas temperature that lies in the range between 13.2 and 22.3 keV at the 90 per cent confidence level, and is larger than 12.1 keV at 3σ level. The existence of such a hot galaxy cluster at redshift of about 0.45 implies an upper limit on the mean mass density in the Universe, Ω_m , of 0.5.

Combining the *BeppoSAX* estimates for gas temperature and luminosity of the three clusters presented in this work with *ASCA* measurements available in the literature, we obtain a slope of 2.7 in the $L - T$ relation once the physical properties are corrected from the contamination from the central cooling flows.

Key words: galaxies: clustering – X-ray: galaxies.

1 INTRODUCTION

The X-ray emitting gas in clusters of galaxies cools by the emission of energy on a time scale which depends on the temperature and density of the intracluster medium (ICM). Where the density is higher, in the cores of the clusters, the cooling is more efficient and the temperature falls. To support the outer layers of gas, a subsonic flow of gas occurs towards the central region, producing a *cooling flow* that appears in X-rays as an enhancement of the central peak in the surface brightness profile and with a spectrum that presents multiple temperature components.

The stronger the cooling flow, the higher the X-ray luminosity which arises from both the thermal energy lost by the cooling gas and the gravitational work done to maintain the gas at constant pressure. Therefore, to compare global cluster gas properties with theoretical and numerical predictions, that, at present, cannot model the radiative cooling in detail, we need to account fully for the effects of cooling flows on the temperature and luminosity measurements (Fabian et al. 1994, Allen & Fabian 1998, Markevitch 1998).

In this paper, we present data collected with the instruments onboard of the Italian-Dutch satellite *BeppoSAX* for three highly luminous ($L_{\text{bol}} > 10^{45}$ erg s $^{-1}$), hot ($T_{\text{gas}} \gtrsim 10$ keV), distant ($z > 0.2$) clusters of galaxies with large ($\gtrsim 1000 M_{\odot}$ yr $^{-1}$) mass deposition rates in their cores (Allen 2000): RXJ1347-1145, Zwicky 3146 (Z3146) and Abell 2390 (A2390). Using data from both the Low Energy (LECS) and Medium Energy (MECS) Con-

centrator Spectrometer and a joint analysis with the Phoswich Detection System (PDS) data above 10 keV, we show that it is possible to constrain at a high level of significance the hard tail of the bremsstrahlung emission.

All quantities quoted in this paper refer to the following cosmological parameters: $H_0 = 50 h_{50}^{-1}$ km s $^{-1}$ Mpc $^{-1}$, $\Omega_m = 1$, $\Omega_{\Lambda} = 0$.

2 THE SAMPLE

We describe here the characteristics of the three galaxy clusters analyzed in the present study.

RXJ1347-1145 is a lensing cluster found in the *ROSAT* All Sky Survey (Schindler et al. 1995, 1997), with a slightly elongated X-ray structure around a very peaked central emission as it appears in the *ROSAT* HRI image. Analyses of the *ASCA* dataset provide temperature estimates ranging from $9.3^{+1.1}_{-1.0}$ keV (Schindler et al. 1997), when a single temperature model is adopted, to $26.4^{+7.8}_{-12.3}$ keV (Allen 2000), when a multi-phase gas is considered.

Z3146 is the fourth ranked luminous cluster in the *ROSAT* band as reported in the Brightest Cluster Sample (BCS, Ebeling et al. 1998). Its massive cooling flow has been inferred from the strong optical lines and blue continuum exhibited by its central galaxy and has been studied with *ROSAT* HRI (Edge et al. 1994). Allen (2000)

arXiv:astro-ph/0010162v2 11 Jan 2001

quotes an *ASCA* estimate of the gas temperature corrected from the cooling flow of $11.3^{+5.8}_{-2.7}$ keV.

A2390 is the sixth ranked luminous cluster in the *ROSAT* band in the northern sky (BCS, Ebeling et al. 1998), has been widely studied in the X-ray waveband (Ulmer et al. 1986, Böhringer et al. 1999) and is optically rich (Abell, Corwin & Olowin 1989, Yee et al. 1996). It presents evidence of strong and weak lensing (Pello et al. 1991, Pierre et al. 1996, Squires et al. 1996). For A2390, Böhringer et al. (1999) measure $kT_{\text{gas}} \sim 9$ keV when an isothermal model is used to fit the *ASCA* data. Once they add a cooling flow component and consider a *ROSAT* PSPC–*ASCA* joint fit, the temperature rises to $11.1^{+1.5}_{-1.6}$ keV. Using the *ASCA* dataset only, Allen (2000) measures $kT_{\text{gas}} = 10.13^{+1.22}_{-0.99}$ keV with a single isothermal model, that rises to $14.5^{+15.5}_{-5.2}$ keV with a cooling flow component included in the spectral fit.

In Table 1, we quote for these three clusters the exposure and net count rates measured in each instrument on board *BeppoSAX*, the Galactic absorption estimated in direction of the X-ray centroid determined from the respective *ROSAT* HRI image (see Fig. 1) and their redshift from literature. Given the assumed cosmology, one arcmin corresponds to 0.408, 0.324, $0.277 h_{50}^{-1}$ Mpc, at the redshift of RXJ1347-1145, Z3146, A2390, respectively.

3 SPECTRAL ANALYSIS

We present the data from the three instruments onboard the Italian-Dutch satellite *BeppoSAX* (Boella et al. 1997): LECS (0.1–4 keV), MECS (1.8–10.5 keV) and PDS (15–200 keV). In Table 1, we present the details of the observations.

Using XSELECT v2.0, we extract the spectra after screening for events without an attitude solution (generally 1 count for every 1,000 good events) from the standard cleaned and linearized event file of LECS and the merged event file collected from units 2 and 3 of the MECS.

For all three clusters, we have selected circular regions with radii of 8 arcmin around the source in the LECS image and 6 arcmin in the MECS image. These regions should contain more than 95 per cent of the flux observed in the MECS and about 90 per cent of that collected from the LECS, given the standard calibration files for point sources (see below for the calibration files adopted in the present analysis).

Using similar regions in detector coordinates, background spectra were extracted from the MECS23_bkg.evt file, a 475 ksec exposure of blank fields at high Galactic latitude. Following the procedure described in Fiore, Guainazzi & Grandi (1999), we have checked that the count rates in regions of the source field far away from the two calibration sources, the MECS strongback and any evident serendipitous source are consistent with the count rates measured in the same regions (in detector coordinates, DETX and DETY) in the blank-field.

For the spectral analysis, we have made use of the calibration files released on September 1997 from the SAX-SDC, specifically the redistribution matrix file `lecs_sep97.rmf` and `mecs1_sep97.rmf`, and the ancillary response file `lecs_130_124_8_sep97.arf` and `mecs23_6_sep97.arf`, for the LECS and MECS, respectively. Moreover, we have used the SAXDAS routine *lemat* to obtain both the RMF and ARF files for the three datasets simulating the extend emission of the cluster with $n \sim 100$ point sources each with an estimated contribution to the X-ray flux determined by the opportunely rebinned image in RAW coordinates.

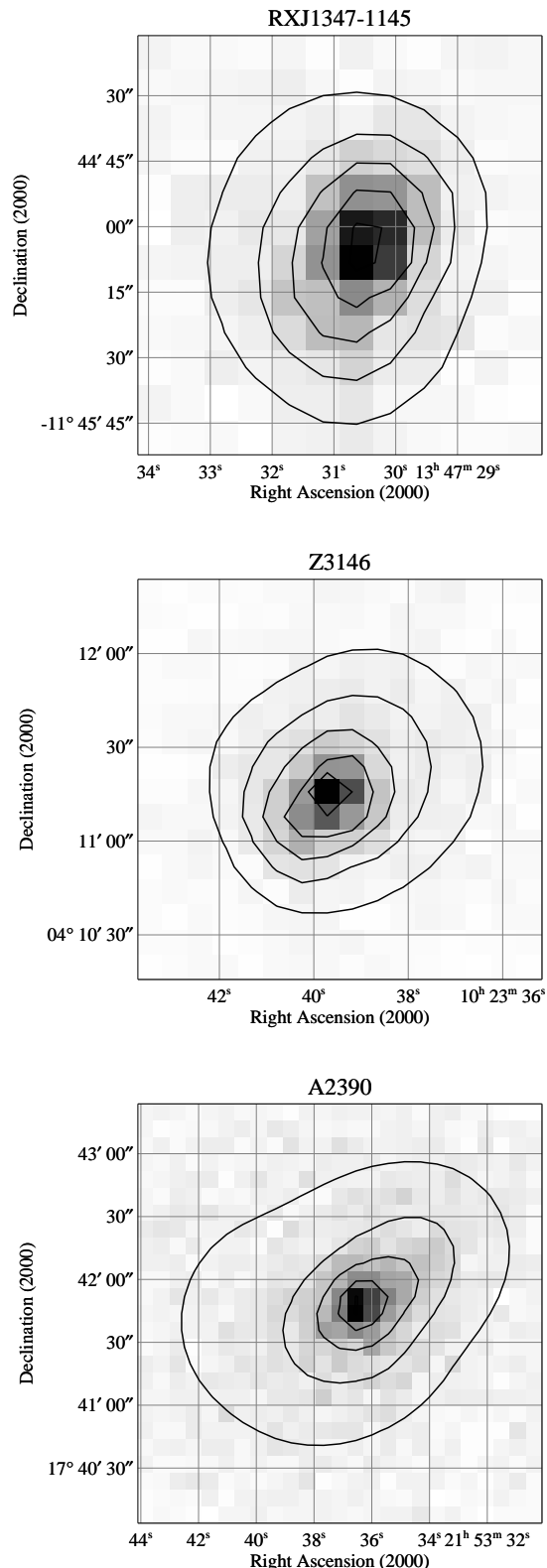


Figure 1. Raw *ROSAT* HRI images with pixel-width of 5 arcsec for the three clusters in our sample, with adaptively smoothed contours, obtained using a Gaussian kernel that encloses a number of counts equal to five times the local background, overlaid.

Table 1. Summary of the *BeppoSAX* observations of the clusters in our sample. The Galactic absorption N_{H} is in unit of 10^{20} cm^{-2} (Dickey & Lockman 1990). References for the redshift: [1] Schindler et al. 1995, [2] Allen et al. 1992, [3] Yee et al. 1996.

Cluster	RA, Dec (2000) hms, deg	z	N_{H}	date	LECS (0.1–4 keV)		MECS (2–10.3 keV)		PDS (13–60 keV)	
					Exp. (ksec)	$10^{-2} \text{ cts s}^{-1}$	Exp. (ksec)	$10^{-2} \text{ cts s}^{-1}$	Exp. (ksec)	$10^{-2} \text{ cts s}^{-1}$
RXJ1347-1145	13 47 31.0, -11 45 11	0.4510 [1]	4.8	2000 Jan 25	28.6	5.3 ± 0.1	73.2	9.9 ± 0.1	36.5	4.0 ± 2.6
Z3146	10 23 40.0, +04 11 11	0.2906 [2]	3.0	1999 Dec 07	13.1	6.2 ± 0.2	38.4	9.3 ± 0.2	17.9	8.2 ± 3.6
A2390	21 53 36.8, +17 41 44	0.2279 [3]	6.8	1999 May 28	33.0	9.0 ± 0.2	76.1	16.5 ± 0.2	35.4	2.1 ± 2.4

The counts were grouped to a minimum of 25 per bin in order that the χ^2 statistic could be applied in the fitting analysis.

In the process of fitting the spectra simultaneously, we have left free the intercalibration constant of the spectral normalization in the LECS with respect to that in the MECS, used as reference. This value varies between 0.71 and 0.73 when an effective area appropriate for a point-source is used in fitting the LECS data. This is in agreement with the present absolute calibration of the two instruments. When the more appropriate ARF file created with *lemat* is used, the intercalibration constant is about 1 for all the best-fit results.

The PDS background-corrected spectra were retrieved from the on-line SDC archive and analyzed using the redistribution matrix file `pds_256_aug97_fix_jan98.rmF`. We group the PDS counts according to the grouping file provided by SDC. The PDS vs. MECS normalization factor was fixed to 0.86. No differences are observed between PDS spectra that do or do not include corrections due to applying a crystal-temperature-dependent Rise-Time threshold.

We fit the spectra using the photoelectric absorption model that adopts the cross-sections calculated by Balucinska-Church and McCammon (1992), in front of a MEKAL emission model (Kaastra 1992, Liedhal et al. 1995) in XSPEC (version 11.0.1, Arnaud 1996). The absorption is fixed to the Galactic value quoted in Table 1 obtained from the $0.675^\circ \times 0.675^\circ$ pixel HI map of Dickey & Lockman (1990). The results of the fitting analysis are presented in Table 2 and shown in Figure 2. As comparison, we quote in Table 2 the results for a thermal fit to the MECS data only.

In the same Table, we also present the results obtained from fitting two further models that include an additional contribution to the single-phase plasma: (i) a power-law that can take into account any non-thermal contamination from an unresolved active galaxy; (ii) an intrinsically absorbed cooling flow component which can model the emission from the central multi-phase gas (see also discussion for the *ASCA* data in Allen & Fabian 1998). The aim in fitting these models is to check the robustness of the gas temperature estimates against any additional contribution to the thermal emission. We note, however, that the LECS, which provides data in the soft X-ray part of the spectrum and is used to constrain the intrinsic absorption and the normalization of the cooling flow component, has an energy resolution (FWHM) of about 11 per cent at 3 keV, that is comparable to *ASCA* Gas scintillation Imaging Spectrometers (GIS) but is poorer by a factor of 4 than the Solid state Imaging Spectrometers (SIS), which also has an effective area larger by a factor of 10 than the LECS. Therefore, any constraint on the modeling of the low-energy spectrum obtained through the “1T+CF” model will be less tight of that provided *ASCA* data (see Allen 2000). In our analysis, we placed lower and upper limit on the intrinsic cluster absorption of 10^{19} and 10^{22} cm^{-2} respectively. We flag as *unc* the values which are unconstrained within these bands by our analysis.

The quoted pseudo-bolometric luminosity is estimated over the energy range 0.01–100 keV for the “1T+CF” model.

Generally, all of the spectral fits provide an acceptable reduced χ^2 . We discuss in the next subsection the results obtained from both the “1T” and “1T+CF” model. Regarding the “1T+pow” model, we note that only A2390 shows a constrained contribution from a power-law component with a luminosity less than $10^{45} \text{ erg s}^{-1}$ (2–10 keV) and a photon index of $2.69_{-1.31}^{+2.68}$ consistent with the typical value for active galaxies (e.g. Nandra et al. 1997). Both RXJ1347-1145 and Z3146 do not show reasonable values to model the power-law component. For reference, we quote in Table 2 the best-fit results obtained for the three clusters in exam with the “1T+pow” model and fixing the photon index to 2 (Nandra et al. 1997).

3.1 Comparison with *ASCA* and *ROSAT* results

All of the clusters in our sample were observed with both the *ASCA* (Tanaka et al. 1994) and *ROSAT* (Trümper 1983) satellites. We discuss below the previous estimates of the gas luminosity and temperature in comparison to the results presented in this work.

- **RXJ1347-1145.** Schindler et al. (1997) estimate a luminosity of $76 \times 10^{44} \text{ erg s}^{-1}$ in the 2–10 keV *ASCA* /GIS band. This measurement is about 20 per cent lower than the value estimated from the *ASCA* /GIS3 for the same dataset by Allen (2000; $L_{44, 2-10\text{keV}} \sim 93.5$, where hereafter L_{44} is the luminosity in unit of $10^{44} \text{ erg s}^{-1}$). From the fit of the MECS spectrum alone, we measure an intermediate value between the two *ASCA* estimates of $83.5 \times 10^{44} \text{ erg s}^{-1}$.

Schindler et al. (1997) also report a luminosity of 7.3 and $\sim 21 \times 10^{45} \text{ erg s}^{-1}$ with *ROSAT* /HRI in the 0.1–2.4 keV and bolometric bands, respectively. Whereas the extrapolation of our 1T best-fit provides only ~ 70 per cent of the *ROSAT* flux in the 0.1–2.4 keV band, the bolometric value is in good agreement with the result obtained from the 1T+CF model applied to the joint analysis of the 3 *BeppoSAX* instruments and about 7 per cent lower than the estimate in Allen (2000).

More controversial is the case for the gas temperature. While the estimate in Allen (2000) obtained from fitting simultaneously the 0.6–10 keV SIS and 1–10 keV GIS data is in agreement with the best-fit value of about 14 keV within the 90 per cent confidence interval, the value of $9.3_{-1.0}^{+1.1} \text{ keV}$ (90 per cent confidence level) quoted in Schindler et al. (1997) can be excluded from the *BeppoSAX* data at 99.99 per cent confidence level. In fact, from our analysis, the 3σ (99.73 per cent) lower limit is given by a temperature of 12.1 keV.

We show in Fig. 3 the residuals produced from the *BeppoSAX* data when the model of Schindler et al. (1997) is used. In particular, it seems that most of the residuals appear at energies below ~ 1 keV and above ~ 8 keV, in spectral region not well covered from the selected energy range in their *ASCA* analysis of 0.7–9 keV.

- **Z3146.** The estimated intrinsic rest-frame luminosity from the

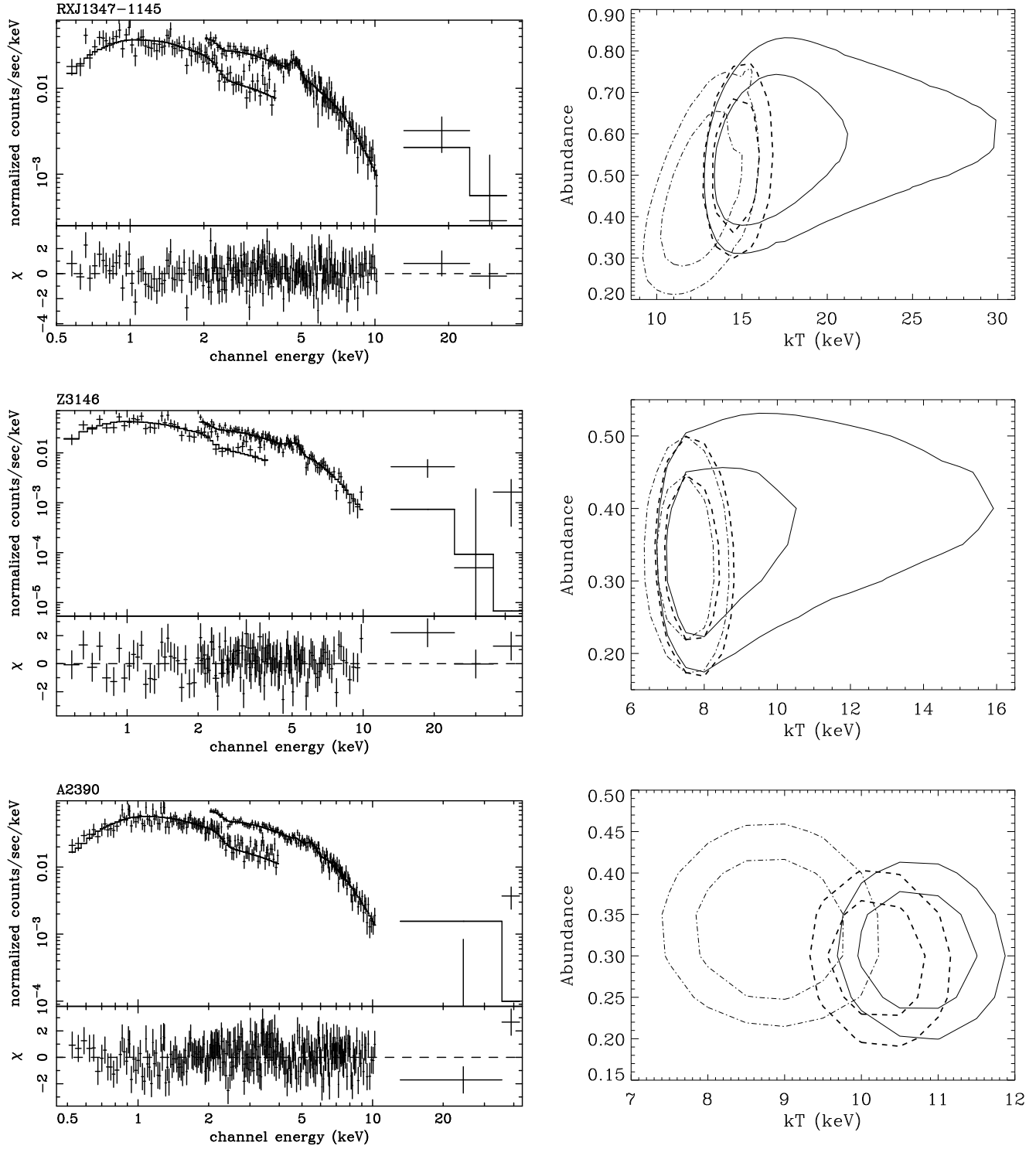


Figure 2. (Left) Data and best-fit folded MEKAL model absorbed by Galactic absorption. We plot the result of the joint fit analysis of the LECS, MECS and PDS data and the corresponding residuals in terms of σ . (Right) Confidence contours ($\Delta\chi^2 = 2.30, 4.61$ corresponding to a confidence level of 68.3 and 90 per cent, respectively, for 2 degrees of freedom) relative to the best-fit on the two interesting parameters, the metal abundance and the gas temperature. The solid line encircles the accepted values given a thermal plus cooling flow component; the dashed line represents the best-fit results obtained with a single thermal component; the dot-dashed line is obtained using a thermal component plus an absorbed power law (see Table 2).

Table 2. Best-fit spectral parameters. The errors are at 90 per cent confidence limit. The absorption is fixed to the respective Galactic value and the redshift to the optical estimate (cf. Table 1). The model used in XSPEC is `phabs(mekal)` (1T), `phabs(mekal+zphabs(powerlaw))` (1T+pow), `phabs(mekal+zphabs(cfmodel))` (1T+CF). The column “Prob” gives the null hypothesis probability that the fit is acceptable. The column “ \dot{M} -pow” quotes the deposition rate for the 1T+CF model, the photon index of the power law for the 1T+pow model. The column “ $L_{2-10\text{keV}} - L_{\text{bol}}$ ” quotes either the luminosity in the 2–10 keV band for the fit on only MECS data or the expected contribution in the same band from any power law component (given the nominal values of the fit and upper limit at 90 per cent confidence level for a fixed photon index of 2) or the bolometric value calculated from the 1T+CF model. Note that *unc* means unconstrained.

data	Model	kT keV	abundance Z/Z_{\odot}	χ^2_{ν} (d.o.f.)	Prob	ΔN_{H} 10^{21} cm^{-2}	\dot{M} -pow	$L_{2-10\text{keV}} - L_{\text{bol}}$ $10^{44} \text{ erg s}^{-1}$
RXJ1347-1145								
only MECS	1T	$14.25^{+1.79}_{-1.48}$	$0.51^{+0.19}_{-0.17}$	0.989 (131)	0.52	–	–	83.5
LECS + MECS + PDS	1T	$14.48^{+1.76}_{-1.46}$	$0.52^{+0.19}_{-0.18}$	0.993 (207)	0.52	–	–	–
	1T+pow	$12.64^{+2.58}_{-2.65}$	$0.46^{+0.22}_{-0.19}$	0.990 (205)	0.53	$103.4^{+475.0}_{-81.1}$	2 (fixed)	(14.2, < 30.2)
	1T+CF	$15.88^{+6.47}_{-2.66}$	$0.55^{+0.21}_{-0.19}$	0.999 (205)	0.49	unc	< 1999	204.0
Z3146								
only MECS	1T	$7.26^{+0.90}_{-0.75}$	$0.33^{+0.13}_{-0.12}$	0.904 (97)	0.74	–	–	32.4
LECS + MECS + PDS	1T	$7.60^{+0.92}_{-0.77}$	$0.33^{+0.13}_{-0.12}$	0.992 (141)	0.51	–	–	–
	1T+pow	$7.44^{+0.95}_{-0.85}$	$0.33^{+0.13}_{-0.12}$	0.976 (139)	0.57	> 976.8	2 (fixed)	(49.4, < 106.8)
	1T+CF	$7.75^{+3.47}_{-0.86}$	$0.33^{+0.14}_{-0.12}$	1.003 (139)	0.47	unc	< 1267	69.6
	1T+CF	$7.75^{+3.47}_{-0.86}$	$0.33^{+0.14}_{-0.12}$	1.003 (139)	0.47	unc	< 1267	69.6
A2390								
only MECS	1T	$9.76^{+0.76}_{-0.68}$	$0.30^{+0.08}_{-0.08}$	0.991 (142)	0.52	–	–	34.7
LECS + MECS + PDS	1T	$10.17^{+0.77}_{-0.69}$	$0.29^{+0.09}_{-0.08}$	1.074 (263)	0.20	–	–	–
	1T+pow	$8.79^{+1.23}_{-1.08}$	$0.33^{+0.05}_{-0.09}$	1.039 (261)	0.32	$30.8^{+18.6}_{-13.1}$	2 (fixed)	(7.8, < 11.6)
	1T+CF	$10.67^{+0.91}_{-0.80}$	$0.31^{+0.08}_{-0.08}$	1.058 (261)	0.25	unc	522^{+308}_{-337}	78.3
	1T+CF	$10.67^{+0.91}_{-0.80}$	$0.31^{+0.08}_{-0.08}$	1.058 (261)	0.25	unc	522^{+308}_{-337}	78.3

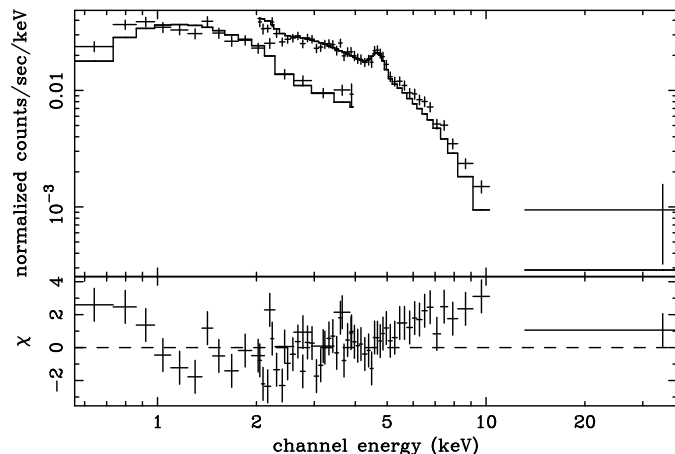


Figure 3. The best-fit model in second line of Table 1 in Schindler et al. (1997) is here considered: $kT = 9.3$ keV, $N_{\text{H}} = 10^{21} \text{ cm}^{-2}$, $Z = 0.32Z_{\odot}$. Only the normalization is left free to vary. The rebinning is done for presentation purpose.

RASS (0.1–2.4 keV, Ebeling et al. 1998) is $26.5 \times 10^{44} \text{ erg s}^{-1}$. Using the same spectral model of Ebeling and collaborators, we calculate a $L_{44,0.1-2.4\text{keV}}$ of 20.0. Extrapolating the results of our 1T model, we measure $25.8 \times 10^{44} \text{ erg s}^{-1}$. Thus, there is evidence for a slight mismatch in the spectrum shape between *ROSAT* and *BeppoSAX*, despite a general agreement in the normalization.

In the 2–10 keV band, the fit of the MECS spectrum provides a luminosity of $32.4 \times 10^{44} \text{ erg s}^{-1}$, 13 per cent lower than the estimate from *ASCA* /GIS3 in Allen (2000).

Regarding the plasma temperature, our estimates are consistent within the 90 per cent confidence level with the results in Allen (2000).

- **A2390.** Böhringer et al. (1999) fit both *ROSAT* /PSPC and *ASCA* /GIS data. They measure a luminosity of 27 (0.1–2.4 keV) and ~ 35 (2–10 keV) $10^{44} \text{ erg s}^{-1}$. Ebeling et al. (1998) quote an intrinsic luminosity of $21.4 \times 10^{44} \text{ erg s}^{-1}$ from the *ROSAT* All Sky Survey. Extrapolating to the 0.1–2.4 keV band the fit on our dataset, we obtain $L_{44} = 23.7, 24.2$ using the spectral model in Ebeling et al. (1998) and our best-fit 1T model, respectively, in good agreement with the *ROSAT* estimates.

Allen (2000) quotes a 2–10 keV *ASCA* /GIS3 luminosity of $41.0 \times 10^{44} \text{ erg s}^{-1}$, that is about 17 per cent higher than both the estimate of Böhringer et al. (1999) and our measure from MECS data only of $34.7 \times 10^{44} \text{ erg s}^{-1}$.

The gas temperature quoted in both Allen (2000) and Böhringer et al. (1999), and obtained from analysis of *ASCA* data, are consistent within the 90 per cent confidence limits with the values measured from the joint LECS-MECS-PDS fit.

In conclusion, our results point to a general 10 per cent systematic disagreement among the *ASCA*, *ROSAT* and *BeppoSAX* flux calibrations. It is worth noting that Grandi and Guainazzi show in the 1999 report on the *BeppoSAX* - *ASCA* intercalibration using 3C273 that GIS3 provides a normalization of the continuum higher by a factor between 9 and 15 per cent than the corresponding value estimated in the same energy band with MECS for quasi-simultaneous data acquired in 1996 and 1998.

4 A COOLING-FLOW CORRECTED L-T RELATION

The relations between the measured (e.g. gas temperature and luminosity) and derivative (e.g. total gravitating mass) quantities determined from X-ray observations is a basic step in constraining cosmological parameters through the cluster mass function.

The observed values of the intracluster gas luminosity and

temperature are correlated due to the fact that the luminosity depends on the cluster baryon fraction and the temperature is a direct measure of the potential well of the dark halo.

In fact, the luminosity, L , goes like $\Lambda(T)n_{\text{gas}}^2 r^3 \sim \Lambda(T)T^{3/2}(1+z)^{3/2}(\Omega_m/\Omega_m(z))^{1/2}$, where we have considered that (i) the gas fraction ratio is constant with redshift, (ii) the dark matter density evolves like $(1+z)^3$, and (iii) the equation of the hydrostatic equilibrium, $M_{\text{tot}} \sim rT$, holds.

Considering that bremsstrahlung emission is the dominant emission process in clusters with $kT > 2$ keV, the cooling function, $\Lambda(T)$, is then proportional to $T^{1/2}$ and, consequently, the bolometric luminosity is proportional to the square of the temperature, $L \sim T^2$. However, this is only valid for a sufficiently hot cluster where the ambient luminosity and temperature are well determined above any contamination, like the excess in cool emission present in the core of cooling flow clusters (e.g. Fabian et al. 1994, Allen & Fabian 1998, Markevitch 1998).

The three clusters presented in this work are among the most luminous known and are affected by the presence of the massive central cooling flows. Therefore, it is worth considering where they lie in the $L - T$ plot once we take into consideration the best-fit results of the ‘‘1T+CF’’ model. We add these results to a list of *ASCA* measurements of bolometric luminosity and temperature obtained from literature and corrected for the contamination from cooling flows, either by including a cooling flow model in the spectral analysis (like we have done in the present analysis; cf. also Allen & Fabian 1998) or excluding the central emission to compose the analyzed spectrum (e.g. Markevitch 1998).

The final sample is plotted in Fig. 4 and contains 64 entries. Of these, 3 are in common between our sample and the one of Allen and collaborators (A2390, Z3146, RXJ1347-1145), five (A478, A1795, A2029, A2142, A2319) are analyzed both in Allen & Fabian (1998) and in Markevitch (1998).

The physical values of the clusters in the combined sample range between 2.8×10^{44} (A2657) and 2×10^{46} (RXJ1347-1145) erg s^{-1} in bolometric luminosity (the median of the distribution is 3.0×10^{45} erg s^{-1}), between 3.5 (A1736) and 15.9 (RXJ1347-1145) keV in temperature (median: 8 keV), between 0.04 (A2657) and 0.451 (RXJ1347-1145) in redshift (median: 0.085).

To investigate the behavior of the $L - T$ relation, we use the following linear fit

$$\log Y = \log a + b \log X, \quad (1)$$

where $Y = L_X/(10^{44} h_{50}^{-2} \text{ erg s}^{-1})$ and $X = T_{\text{gas}}/(10 \text{ keV})$, and we use the downhill simplex method implemented in the *amoeba* routine to minimize the following χ^2 merit function (Press et al. 1992):

$$\chi^2(a, b)_i = \sum_N \frac{(\log Y - \log a - b \log X)^2}{\epsilon_Y^2 + b^2 \epsilon_X^2} \quad (2)$$

for each of the different datasets i considered in our sample. In the equation above, $\epsilon_Y = \sigma_L/L_X$ and $\epsilon_X = \sigma_T/T_{\text{gas}}$. We assume a 10 per cent uncertainty on the luminosity measurements (i.e., $\epsilon_Y = 0.1$) and σ_T equal to the maximum of the 68.3 per cent confidence asymmetric errors on the temperature.

In particular, combining several different datasets, we follow the indications in Lahav et al. (2000) for minimizing a ‘‘weighted’’ merit function

$$C = \sum_i N_i \ln (\chi^2(a, b)_i), \quad (3)$$

where N_i is the number of data present in the dataset i . This for-

malism allows us to consider some effective Hyper-Parameters, $hp = N_i/\chi^2(a, b)_i$, that provide a diagnostic on the systematic effects (more relevant for low hp) of that specific dataset in the overall modeling. Considering this, the *BeppoSAX* data are better modelled than the other two datasets ($hp \sim 3$ vs. 0.2).

The errors on the best-fit parameters are estimated from 500 bootstrap replications of the fit. In Table 3, we show both the best-fit parameters a and b and the values that characterize their distribution after 500 bootstraps (i.e., the median and the 16 and 84 percentile that corresponds to the lower and upper 1 σ level in a Gaussian distribution).

Here we note that the computation of the physical properties presented in the present work follows the technique used in Allen (2000) and differs from the analysis done by Markevitch in the fact that we try to model spectrally the emission from the core, whereas Markevitch cuts the core emission from the spectral analysis and extrapolates the contribution from the core to the total luminosity from the external emissivity. To take into account the different way in which the bolometric luminosity is estimated, we leave free the normalization, a , in the $L - T$ relation in eqn. 1 when we perform a linear fit in each dataset. Only the slope parameter is linked among the three datasets.

Combining the three datasets, we observe a slope in the $L - T$ relation of about 2.7. From the distribution of the best-fit values after bootstrap resampling, we are still $\sim 4\sigma$ far (too steep) from the value of 2 predicted from the simple gravitational collapse of plasma in a cluster dark matter.

This result is consistent, within 1σ , among the three different datasets here considered and with the Bayesian analysis applied to the Allen (2000)’s and Markevitch (1998)’s sample by Reichart, Castander & Nichol (1999).

5 DISCUSSION AND CONCLUSIONS

From the *BeppoSAX* observation, we can constrain the ambient temperature in the clusters of galaxies RXJ1347-1145, Z3146 and A2390 with a relative uncertainty of (17/41), (11/41), (7/9) per cent in the (lower/upper) boundary (at the 90 per cent confidence level) respectively, when a cooling flow model is included in the spectral analysis.

Although the instrument characteristics of *BeppoSAX* do not allow us to constrain firmly any absorption intrinsic to the cluster atmosphere and/or the normalization of the emission from the central cooling gas, the measurements of the ambient gas temperature are in agreement, within the 90 per cent confidence level, with the results from the analysis of *ASCA* data in Allen (2000). In particular, the plasma temperature in RXJ1347-1145 appears well defined between 13.2 and 22.3 keV (90 per cent confidence level) and above 12.1 keV at the 3σ level. This measurement of the temperature is in good agreement with an independent estimate of 16.2 (± 3.8 , 1σ level) keV obtained from the observed X-ray gas density and the measured Sunyaev-Zeldovich (1972) distortion of the cosmic microwave background in the direction of RXJ1347-1145 (Pointecouteau et al. 1999; see also Komatsu et al. 1999).

Following the arguments of many authors (e.g. Bahcall & Fan 1998, Donahue et al. 1999, Henry 2000) the existence of such a hot cluster at redshift 0.45 is highly unlikely in an Einstein - de Sitter universe. We can estimate this probability, calculating the expected evolution of collapsed structures with a given minimum mass according to the Press-Schechter (1974) formalism. Integrating the number of collapsed objects with gravitating mass above that cor-

Table 3. Best-fit results on the luminosity–temperature relation for the data in our sample with median values of $L = 30.0 \times 10^{44} \text{ erg s}^{-1}$ and $T = 8.0 \text{ keV}$. The first two columns state the sample analysed and the number of objects in exam. The third column indicates the number of objects considered in each subsample and the measured χ^2 for the global best-fit. The scatter in the fourth column is defined as $[\sum(\log Y - \log a - b \log X)^2 / N]^{1/2}$, where $Y = L_X / (10^{44} h_{50}^{-2} \text{ erg s}^{-1})$ and $X = T_{\text{gas}} / (10 \text{ keV})$. Note that the scatter along the X-axis can be estimated as $\sigma_{\ln X} = \sigma_{\ln Y} / b$. In the last column, we quote the best-fit slope after applying the technique described in Section 4, and the median and 1σ error after 500 bootstrap replications.

cut	N data	N sample (χ^2)	scatter	b
only <i>BeppoSAX</i> data	3	3 (0.9)	0.327	2.21 (1.50 \pm 1.13)
only Allen (2000)	30	30 (141.3)	0.512	2.41 (2.41 \pm 0.35)
only Markevitch (2000)	31	31 (108.7)	0.240	2.78 (2.78 \pm 0.16)
all	64	3 (1.0), 30 (146.8), 31 (109.9)	0.437	2.69 (2.76 \pm 0.17)
$L > 10 \times 10^{44} \text{ erg s}^{-1}$	53	3 (1.0), 30 (141.5), 20 (71.0)	0.420	2.45 (2.57 \pm 0.29)
$T > 6 \text{ keV}$	46	3 (1.2), 25 (86.0), 18 (61.6)	0.388	2.72 (2.87 \pm 0.30)

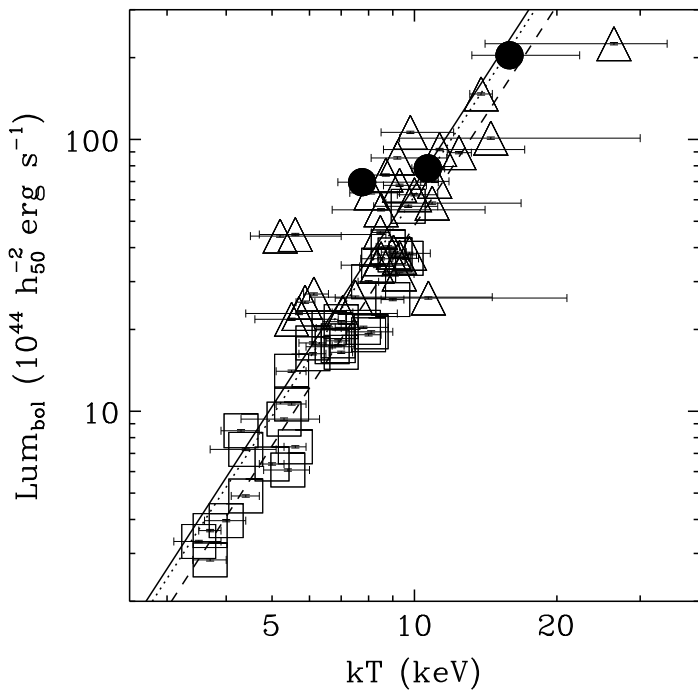


Figure 4. The observed luminosity–temperature relation from *BeppoSAX* and *ASCA* data with the best-fit result obtained for the 64 clusters in our sample. The *solid dots* represent the *BeppoSAX* results for RXJ1347-1145, Z3146 and A2390. The *squares* are from Markevitch (1998). The *triangles* are from Allen (2000). All the estimated temperatures are corrected for the presence of the cooling flow. The error bars are 90 per cent confidence limit. The solid, dotted, dashed lines are the best-fits obtained fixing to a common value the slope and leaving free the normalizations for the objects in the *BeppoSAX*, Allen (2000) and Markevitch (1998) samples, respectively.

responding to a temperature of 15.9 keV over the redshift range of 0.4 – 0.5, and requiring *at least* the existence of RXJ1347-1145, the single detection provides a stringent upper limit of $\Omega_m \lesssim 0.43$. Considering also the lower and upper end of the range of the acceptable gas temperature of 13.2 and 22.3 keV, with the 90 per cent uncertainty on the single detection, we constrain the cosmological parameter Ω_m between 0.25 and 0.70 (cf. Fig. 5).

Future *Chandra* and *XMM* observations of these highly luminous clusters of galaxies at intermediate redshift will resolve spa-

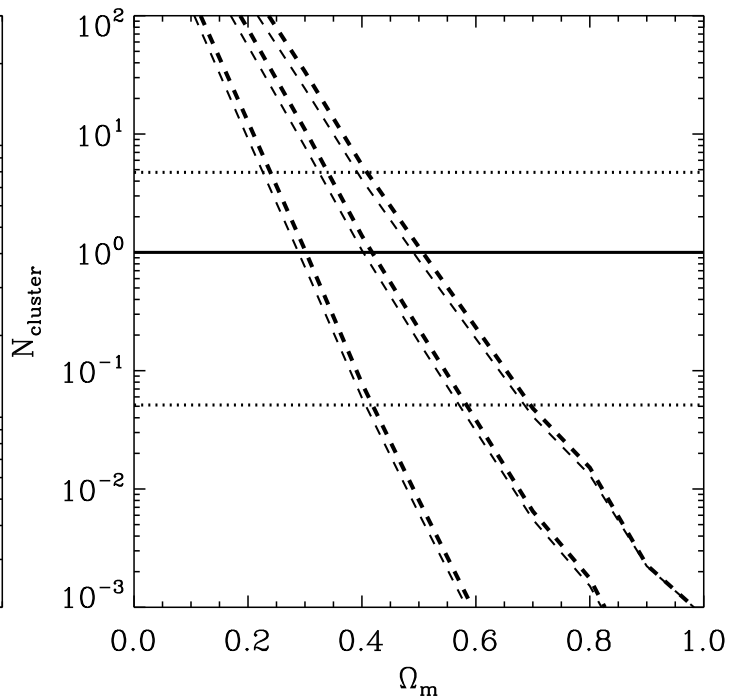


Figure 5. The expected number density of clusters with gas temperature larger than 13.2, 15.9, 22.3 keV (from right to left in the figure, respectively; cf. Table 2 for the constraint on the gas temperature of RXJ1347-1145) in the redshift interval [0.4, 0.5]. The dashed lines represent the distribution in a “ $\Omega_m + \Omega_\Lambda = 1$ ” Universe (thick) and in an open Universe (thin). The error bars, around the observed value of 1 cluster with the given characteristics, are at the 90 per cent level of confidence, according to the Poisson single-sided distribution tabulated in Gehrels (1986).

tially the profiles of the gas temperature, abundance and deposition rate.

ACKNOWLEDGEMENTS

This paper has made use of linearized event files produced at the *BeppoSAX* Science Data Center. We thank T. Oosterbroek and A. Parmar for their help in using the SAXDAS routine *lemat*. The referee, A. Edge, is thanked for his suggestions in improving the

presentation of this work. We acknowledge the support of the Royal Society.

REFERENCES

- Abell G.O., Corwin H.G., Olowin R.P., 1989, *ApJS*, 70, 1
- Allen S.W., 1998, *MNRAS*, 296, 392
- Allen S.W., Fabian A.C., 1998, *MNRAS*, 297, L57
- Allen S.W., 2000, *MNRAS*, 315, 269
- Arnaud K.A., 1996, "Astronomical Data Analysis Software and Systems V", eds. Jacoby G. and Barnes J., *ASP Conf. Series* vol. 101, 17
- Bahcall N. A., Fan X., 1998, *ApJ*, 504, 1
- Balucinska-Church M., McCammon D., 1992, *ApJ*, 400, 699
- Boella G., Butler R.C., Perola G.C., Piro L., Scarsi L., Bleeker J.A.M., 1997, *A&AS*, 112, 299
- Böhringer H., Tanaka Y., Mushotzky R.F., Ikebe Y., Hattori M., 1999, *AA*, 334, 789
- Dickey J.M., Lockam F.J., 1990, *Ann. Rev. Ast. Astr.*, 28, 215
- Donahue M., Voit G.M., Scharf C.A., Gioia I.M., Mullis C.R., Hughes J.P., Stocke J.T., 1999, *ApJ*, 527, 525
- Ebeling H., Edge A.C., Böhringer H., Allen S.W., Crawford C.S., Fabian A.C., Voges W., Huchra J.P., 1998, *MNRAS*, 301, 881
- Edge A.C., Fabian A.C., Allen S.W., Crawford C.S., White D.A., Böhringer H., Voges W., 1994, *MNRAS*, 270, L1
- Fabian A.C., Crawford C.S., Edge A.C., Mushotzky R.F., 1994, *MNRAS*, 267, 779
- Fiore F., Guainazzi M., Grandi P., 1999, *Cookbook for BeppoSAX NFI Spectral Analysis, version 1.2*, available at <http://www.sdc.asi.it/software/cookbook/>
- Gehrels N., 1986, *ApJ*, 303, 336
- Grandi P., Guainazzi M., 1999, "3C273 *BeppoSAX* -ASCA intercalibration", available at ftp://www.sdc.asi.it/~pub/~sax/~doc/~reports/~asca_sax_crosscal.ps.gz
- Henry J.P., 2000, *ApJ*, 534, 565
- Kaastra J.S., 1992, *An X-Ray Spectral Code for Optically Thin Plasmas* (Internal SRON-Leiden Report, updated version 2.0)
- Komatsu E., Kitayama T., Suto Y., Hattori M., Kawabe R., Matsuo H., Schindler S., Yoshikawa K., 1999, *ApJL*, 516, L1
- Lahav O., Bridle S.L., Hobson M.P., Lasenby A.N., Sodre Jr L., 2000, *MNRAS*, 315, L45
- Liedahl D.A., Osterheld A.L., Goldstein W.H., 1995, *ApJ*, 438, L115
- Markevitch M., 1998, *ApJ*, 504, 27
- Nandra K., George I.M., Mushotzky R.F., Turner T.J., Yaqoob T., 1997, *ApJ*, 477, 602
- Pello R., LeBorgne J.F., Soucail G., Mellier Y., Sanahuja B., 1991, *ApJ*, 366, 405
- Pierre M., LeBorgne J.F., Soucail G., Kneib J.P., 1996, *A&A*, 311, 413
- Pointecouteau E., Giard M., Benoit A., Desert F.X., Aghanim N., Coron N., Lamarre J.M., Delabrouille J., 1999, *ApJL*, 519, L115
- Press W.H., Schechter P., 1974, *ApJ*, 187, 425
- Press W.H., Teukolsky S.A., Vetterling W.T., Flannery B.P., 1992, *Numerical Recipes in Fortran*, Cambridge University Press
- Reichart D.E., Castander F.J., Nichol R.C., 1999, *ApJ*, 516, 1
- Sarazin C.L., 1988, *X-ray emission from clusters of galaxies*, Cambridge University Press
- Schindler S., Guzzo L., Ebeling H., Böhringer H., Chincarini G., Collins C.A., De Grandi S., Neumann D.M., Briel U.G., Shaver P., Vettolani P., 1995, *A&A*, 299, L9
- Schindler S., Hattori M., Neumann D.M., Böhringer H., 1997, *A&A*, 317, 646
- Squires G., Kaiser N., Fahlman G., Babul A., Woods D., 1996, *ApJ*, 469, 73
- Sunyaev R., Zeldovich Y., 1972, *Comments Astrophys. Space Phys.*, 4, 173
- Tanaka Y., Inoue H., Holt S.S., 1994, *PASJ*, 46, L39
- Trümper J., 1983, *Adv. Space Res.*, 2, 142
- Ulmer M.P., Kowalski M.P., Craddock R.G., 1986, *ApJ*, 303, 162
- Yee H.K.C., Ellingson E., Carlberg R.G., 1996, *ApJS*, 102, 289